APPROACH TO DEFINE THE AERODYNAMIC FREE AREA FOR NATURAL SMOKE VENTS IN A CFD SIMULATION ENVIRONMENT

Csaba Szikra[1], Lajos Gábor, Takács PhD[2]

[1]Budapest University of Technology and Economics, Faculty of Architecture,
Department of Building Energetics and Building Services
1-3 Műegyetem rkp.,
Budapest, 1111 Hungary
e-mail: szikra@egt.bme.hu

[2]Budapest University of Technology and Economics, Faculty of Architecture,
Department of Building Constructions
1-3 Műegyetem rkp.,
Budapest, 1111 Hungary
e-mail: ltakacs@epsz.bme.hu

1. ABSTRACT

Provided naturally or mechanically, smoke and heat exhaust from buildings is one of the key application fields of CFD simulations [1] [2]. In an FDS/Pyrosim environment, natural smoke vents may be modelled by simple openings called "Hole" elements, whose sizes are essential in the findings of simulation. In our paper, we propose a method to model natural flat roof ventilators in CFD simulation using a proper size.

2. GEOMETRIC SIZE AND AERODYNAMIC FREE AREA OF NATURAL SMOKE AND HEAT VENTS

2.1. Study of the aerodynamic free area

The key performance indicator of natural smoke and heat vents is their aerodynamic free area, whose quotient with geometric size is referred to as the coefficient of discharge (c_v). In Europe, the aerodynamic free area and the coefficient of discharge is determined by a test described in the standard EN 21101-2 [3]. This test may be performed on full scale or reduced scale models. When testing reduced scale models, flow similarity shall be achieved. This is implemented, when the Reynolds number for a reduced scale and a full scale vent is the same. To achieve the same Reynolds number, usually a model of 1/6 or higher scale is necessary. If aerodynamic similarity validly holds, then lower scales (down to 1/10) may also be used.

The test equipment consist of a settling chamber and a side wind simulator exposing the natural smoke and heat vent to side wind to which the natural smoke and heat vent may be mounted on so as to allow for the mass flow passing through the vent to be established.

Inside the settling chamber, the flow approaching the natural smoke and heat vent is stationary and uniform. This is assured, if the ratio between the geometric cross-section of the vent and the horizontal cross-section of the settling chamber, $A_v/A_{sc} \le 0.15$ and the speed distribution measured in the opening (V_{sc}) (without a vent) varies only $\pm 10\%$ of the average speed in the settling chamber ($V_{m, sc}$).
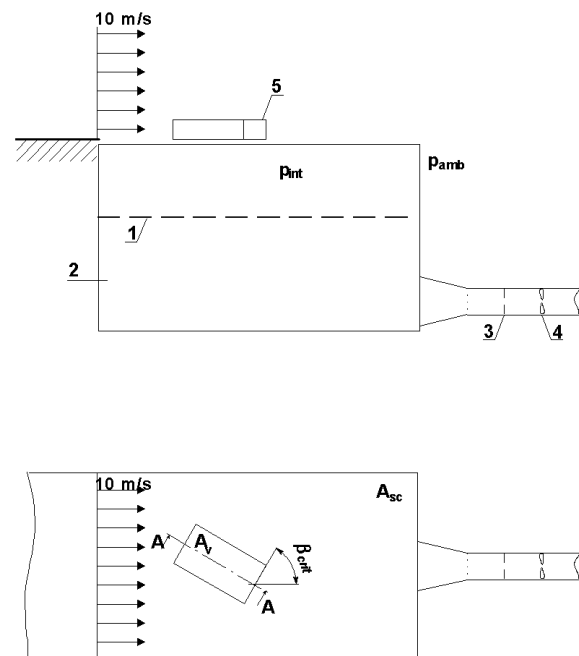
Figure 1: Settling chamber according to EN 12101-2, Annex B, Figure B3 (the tested natural smoke and heat vent is the drawing component No. 5)

2.2. Frequently asked practical questions in relation with the test

The worst problem with the test according to EN 12101-2, Annex 2 is that though the individual aerodynamic free areas resulted for each natural smoke and heat vent are comparable, but in actual practice, natural flat roof smoke and heat vents are installed differently from the test. In general, the settling chamber of the test equipment is usually made of a kind of construction panel of a mere few centimetre thickness; for flat roofs, however, the structure under the natural smoke and heat vent (supporting structure, heat insulation or slope forming for waterproofing, etc.) is at least from 30 to 50 cm or may be even more. For roofs made of trapezoid sheet, secondary supports of the roof ventilators are often placed rather below the trapezoid sheet, then among the wave crests of the trapezoid sheet, whereby the above values of thickness may be further increased.

Natural smoke and heat vents are often installed above spaces with a suspended ceiling so that they are connected to the service area through a smoke-flue in a length of 1 or 2 meters depending on the thickness of the space with the suspended ceiling. The above circumstances may adversely influence the operation of the smoke and heat vent.

3. AERODYNAMIC FREE AREA IN A CFD ENVIRONMENT

The basic idea of our tests is that as verified by testing, the aerodynamic free area and the flow coefficient for natural smoke and heat vents also include the other loss of flow such as friction and reduction of the geometric cross-section in addition to the phenomenon "vena contracta". All these are seen in the following equation:

$$\dot{m}_{ing} = C_v \cdot A_v \cdot v \cdot \rho_{air} = C_v \cdot A_v \cdot \rho_{air} \sqrt{\frac{2 \Delta p_{int}}{\rho_{air}}}$$

The radicant on the right side of this equation derives from the ideal (non-friction) Bernoulli equation, describing the ideal mass flow resulted from the particular pressure difference through an opening. The relationship between the non-friction and real flow is created by the coefficient of discharge (C_v).

With the above equation reduced to the factor C_v and to lower terms by density, the following equation results:

$$C_v = \frac{\dot{m}_{ing}}{A_v \cdot \sqrt{2 \rho_{air} \cdot \Delta p_{int}}}$$

The above equation is suitable to calculate the factor C_v, for which it is necessary to know the static pressure difference between the outer and inner side of the vent (Δp_{int}), as well as the mass flow of the vent ($\dot{m}_{ing}$). In the simulation settling chamber, pressure and flow measuring devices as well as 'slices' are placed.
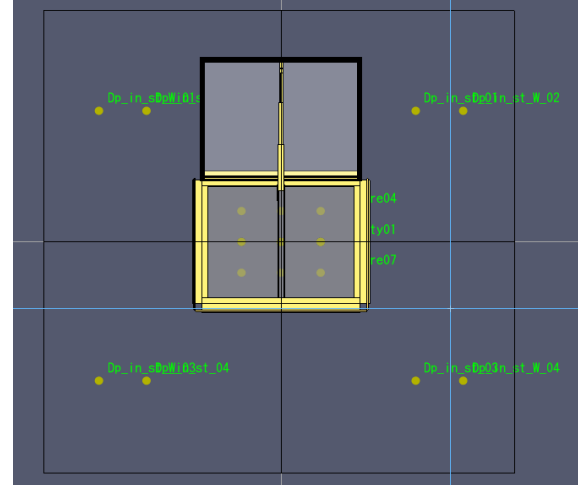
Figure 2: Pressure and flow measuring devices placed in the settling chamber

As seen from experiences, a relatively uniform pressure distribution is resulted in the settling chamber. To provide a uniform speed distribution, a "Vent" element is defined on the lower plane of the settling chamber to regulate the mass flow entering the chamber. In general, 5 cm grid spacing was used to carry out the simulations.
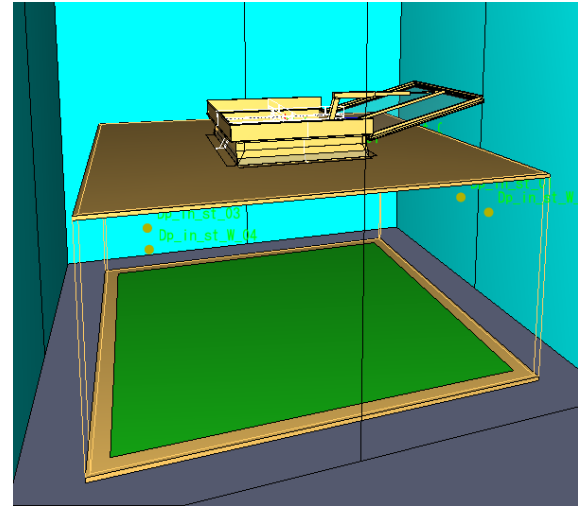
Figure 3: The "Vent" element of 5.5x5.5 cm area, placed in the settling chamber

For the simulation, the Pyrosim environment 2014.1.0331 and the version 6.0.1 FDS was used [4] [5]. In an FDS/Pyrosim simulation environment, when a natural smoke and heat vent is simulated with a "Hole" element, smoke and heat vents are simulated by the simplest sharp corner. However, natural smoke

and heat vents may be designed with footing of many kinds, some examples are shown in Figure 4.
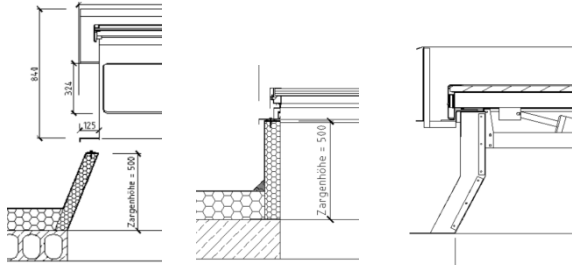
Figure 4: *Natural smoke and heat vents with standard, straight, and angular footing in various size*

As obvious from the foregoing, construction dependent attributes of the footing design and the natural smoke and heat vent (such as floor thickness, safety structures, smoke-flues, etc.) are not taken into account at all or not in full in the CFD simulations. If in the simulation, a natural smoke and heat vent is simulated by a "Hole" element equal to its aerodynamic free area adjusted to the grid, the phenomenon "vena contracta" will be taken into account two times, since this appears when testing the natural smoke and heat vent, as well as the FDS also takes into account when running the simulation. The main goals of our research are as follows:

- is an FDS/Pyrosim environment suitable to simulate the standard test of natural smoke and heat vents,
- how shall the size of a „Hole" element be selected in CFC simulation in the knowledge of the geometric and aerodynamic free area of natural smoke and heat vents.

4. TEST OF THE AERODYNAMIC FREE AREA BY CFD SIMULATION

To decide on any question arising, a test environment has been built in FDS/Pyrosim environment according to EN 12101-2, Annex B. A simple single-wing smoke and heat ventilator of 2,000 x 2,500 mm with wind baffles has been installed on to the settling chamber. The geometrical opening area of this product is 5.0 m^2 with an aerodynamic free area of 3.15 m^2 in case of the specified sizes and conditions, and a coefficient of discharge c_v=0,63.
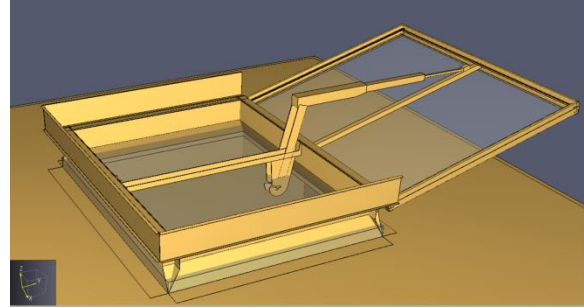
Figure 5: *The natural smoke and heat vent subject to our research illustrated on the settling chamber according to EN 12101-2, Annex B with its movable structure opened in 165° position*

In the first step, the simulation was made without any side wind, taking into account two geometrical cases. In the first case, the vent was installed without modelling the thickness of the floor slab and the thermal insulation. According to EN 12101-2, Annex B, the mass flow was changed during the simulation so as for the overpressure developing in the settling chamber to be between 3-12 Pa in 6 simulation cases. The simulation time was 25 s. During this time, the stationary condition developed. Assuming an ambient temperature of 20 °C, mass flow was calculated from the "Vent supply" speed. As shown in the following table, the speed of the 'Vent supply' was changed from 0.2 to 0.5 m/s. The average speed and the Reynolds number was calculated for the geometrical size of the vent. The grid spacing was basically 5 cm, but the simulation was repeated with a grid spacing of 6,25 cm and 12,5 cm to be comparable with the potential change of the C_v value in function of grid fineness.
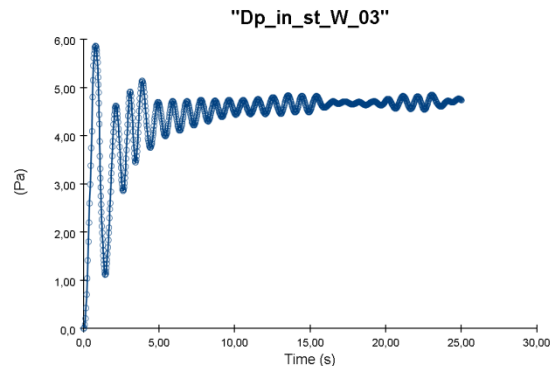
Figure 6: *Time distribution of values of the manometer placed in the settling chamber beside the wall*

File name	MESH cm	Asupp (m2)	vsupp (m/s)	tamb (°C)	ro (kg/m3)	m' (kg/s)	Av (m2)	Vv_average (m/s)	nu (Pa s)	Dv_e (m)	Re_v	Dp_int (Pa)	Cv_0
AM200x250_M05_0_020mps_a	5,0	30,25	0,20	20	1,2042	7,2852	5,0	1,21	1,841E-05	2,0	1,58E+05	1,885058	0,68383
AM200x250_M05_0_025mps_a	5,0	30,25	0,25	20	1,2042	9,1065	5,0	1,51	1,841E-05	2,0	1,98E+05	2,992006	0,67849
AM200x250_M05_0_030mps_a	5,0	30,25	0,30	20	1,2042	10,9278	5,0	1,82	1,841E-05	2,0	2,37E+05	4,295935	0,67948
AM200x250_M05_0_035mps_a	5,0	30,25	0,35	20	1,2042	12,7491	5,0	2,12	1,841E-05	2,0	2,77E+05	5,869612	0,67818
AM200x250_M05_0_040mps_a	5,0	30,25	0,40	20	1,2042	14,5704	5,0	2,42	1,841E-05	2,0	3,17E+05	7,692027	0,67705
AM200x250_M05_0_045mps_a	5,0	30,25	0,45	20	1,2042	16,3917	5,0	2,72	1,841E-05	2,0	3,56E+05	9,775878	0,67564
AM200x250_M05_0_050mps_a	5,0	30,25	0,50	20	1,2042	18,2129	5,0	3,03	1,841E-05	2,0	3,96E+05	12,06646	0,67571

Table 1:   Simulation findings for a construction according to the standard test

The chamber pressure was calculated from integrating the time and space average of the values of the manometer placed near to the four walls. To be noted, these manometers did not indicate any considerable difference in space. The pressure values in time showed some fluctuations. For time integration, the average value was taken into account in a simulation time of 20-25 s.

The C_v value did some changed in the function of time. This change is shown in the function of the average speed developed through the vent (V_v average). From the figure below, it may be established that the C_v factor declines with the increase in mass flow. So, in case of a major flow-through, the effective geometrical cross-section deteriorates, though no significant change occurred in the tested region.
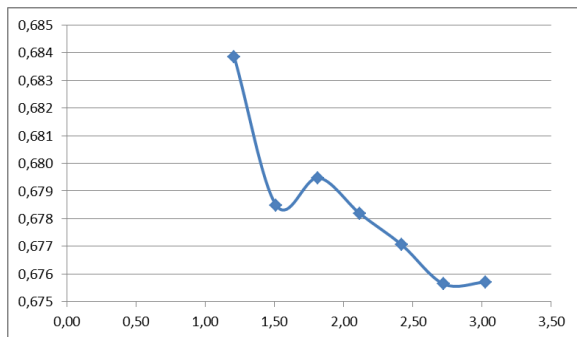
Figure 7:   Change in the C_v value in the function of the average speed calculated for the nominal vent area.

In point of fact, the value of the C_v factor according to standard conditions amounted to 0,677. The manufacturer did not published the test results without side-wind. The test was repeated under the same conditions with the real thickness of a floor slab of a flat roof with thermal insulation.
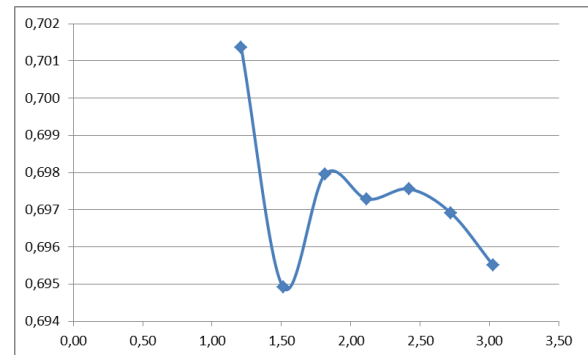
Figure 8:   Change in the C_v value in the function of the average speed calculated for the nominal vent area.

In this case, a slight increase in the effective geometrical area was seen.

File name	MESH cm	Asupp (m2)	vsupp (m/s)	tamb (°C)	ro (kg/m3)	m' (kg/s)	Av (m2)	Vv_average (m/s)	nu (Pa s)	Dv_e (m)	Re_v	Dp_int (Pa)	Cv_0
AM200x250_M05_0_020mps_a_m1	5,0	30,25	0,20	20	1,2042	7,2852	5,0	1,21	1,841E-05	2,0	1,58E+05	1,792026	0,70136
AM200x250_M05_0_025mps_a_m1	5,0	30,25	0,25	20	1,2042	9,1065	5,0	1,51	1,841E-05	2,0	1,98E+05	2,852227	0,69491
AM200x250_M05_0_030mps_a_m1	5,0	30,25	0,30	20	1,2042	10,9278	5,0	1,82	1,841E-05	2,0	2,37E+05	4,071446	0,69796
AM200x250_M05_0_035mps_a_m1	5,0	30,25	0,35	20	1,2042	12,7491	5,0	2,12	1,841E-05	2,0	2,77E+05	5,552409	0,69728
AM200x250_M05_0_040mps_a_m1	5,0	30,25	0,40	20	1,2042	14,5704	5,0	2,42	1,841E-05	2,0	3,17E+05	7,246455	0,69756
AM200x250_M05_0_045mps_a_m1	5,0	30,25	0,45	20	1,2042	16,3917	5,0	2,72	1,841E-05	2,0	3,56E+05	9,188287	0,69691
AM200x250_M05_0_050mps_a_m1	5,0	30,25	0,50	20	1,2042	18,2129	5,0	3,03	1,841E-05	2,0	3,96E+05	11,38916	0,69552

Table 2:   Simulation results in case of a construction with flat roof and heat insulation of actual thickness

File name	MESH cm	Asupp (m2)	vsupp (m/s)	tamb (°C)	ro (kg/m3)	m' (kg/s)	Av (m2)	Vv_average (m/s)	nu (Pa s)	Dv_e (m)	Re_v	Dp_int (Pa)	Cv_0
AM200x250_M12_5_04mps_b	12,5	30,25	0,40	20	1,2042	14,5704	5,0	2,42	1,841E-05	2,0	3,17E+05	8,822784	0,63218
AM200x250_M06_25_04mps_c	6,25	30,25	0,40	20	1,2042	14,5704	5,0	2,42	1,841E-05	2,0	3,17E+05	8,408846	0,64755
AM200x250_M05_0_040mps_a	5,0	30,25	0,40	20	1,2042	14,5704	5,0	2,42	1,841E-05	2,0	3,17E+05	7,692027	0,67705

Table 3:   Simulation results in a heat-insulated construction with various grid spacing

The relationship between grid spacing and effective geometrical cross-section for a construction identical to the standard test was studied.
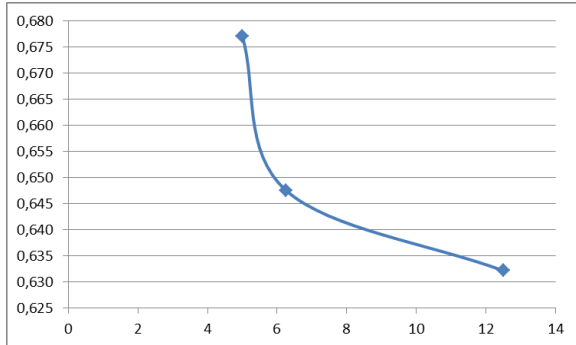
Figure 9: Change in the C_v value in the function of grid spacing

As seen from the above figure, the effective geometrical cross-section increases by grid spacing. For major test objects, the reduction of grid spacing – the increase in cell size – to achieve a reasonable running time will amend the results in favour of safety.
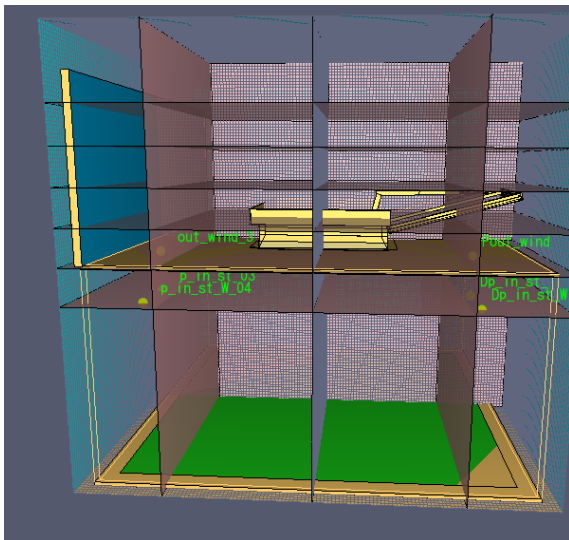
Figure 10: The model used for testing the side-wind

Finally, based on the standard EN 12101-2 B, vent behaviour for side-wind was tested. In the first part of the test with side-wind, we tried to find the most adverse wind direction by using simulation

From the tests, it was established that the pressure conditions prevailing in the settling chamber depend on the assumed wind direction, but the extreme value of this function is highly influenced by the mass flow passing through the vent. To simulate the wind direction, the tangential speed component was used in addition to using blow-in from two directions perpendicular to each other. Finally we found that the worst case is a remarkable direction, the wind direction parallel to the dome open up according to the above figure. In the following step of the test, mass flow was changed according to EN 12101-2, Annex B. Here, six measuring points had to be taken, but in case of the side-wind test, the internal overpressure shall change between 0,5 and 15%, related to the dynamic wind pressure.
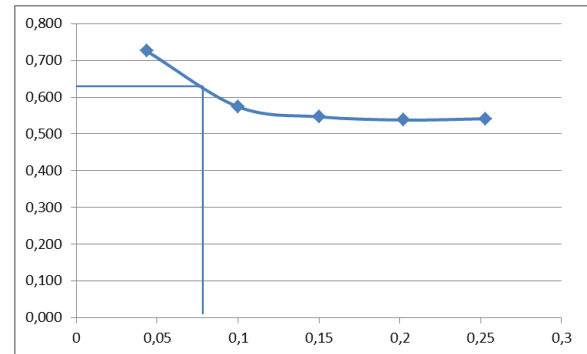
Figure 11: Change in the C_v value in the function of $\Delta p_{int}/P_d$

As seen bellow from the figure and the diagram made of it, the value of the aerodynamic free area depends significantly from the value of $\Delta p_{int}/P_d$. Since assuming 10 m/s wind speed, the value of P_d was constant during the simulation, so changes in the quotient may be originated from the mass flow passing through the vent or from the changes in the average speed. It is seen that the change becomes significant below 2 m/s. In the settling chamber, minor air speeds generate negative C_v values, so the exhaust effect of the wind became dominant. For major mass flows, the wind effect predominated less and less. Based on standard regulations, the C_v values shall be defined by interpolation in case of $\Delta p_{int}/P_d=0.082$.

File name	MESH cm	Asupp (m2)	vsupp (m/s)	tamb (°C)	ro (kg/m3)	m' (kg/s)	Av (m2)	Vv_average (m/s)	nu (Pa s)	Dv_e (m)	Re_v	Dp_int (Pa)	Cv_0	Vn (m/s)	pd (Pa)	dpint min (Pa)	dpint max (Pa)	dpint /pd (Pa)
AM200x250_M05_0_010mps_a_SW2	5,0	30,25	0,10	20	1,2042	3,6426	5,0	0,61	1,841E-05	2,0	7,92E+04	-12,47206		10,00	60,21	0,30	9,03121	-0,20715
AM200x250_M05_0_020mps_a_SW2	5,0	30,25	0,20	20	1,2042	7,2852	5,0	1,21	1,841E-05	2,0	1,58E+05	-0,172716		10,00	60,21	0,30	9,03121	-0,00287
AM200x250_M05_0_025mps_a_SW2	5,0	30,25	0,25	20	1,2042	9,1065	5,0	1,51	1,841E-05	2,0	1,98E+05	2,617494	0,72540	10,00	60,21	0,30	9,03121	0,043474
AM200x250_M05_0_030mps_a_SW2	5,0	30,25	0,30	20	1,2042	10,9278	5,0	1,82	1,841E-05	2,0	2,37E+05	6,02182	0,57391	10,00	60,21	0,30	9,03121	0,100017
AM200x250_M05_0_035mps_a_SW2	5,0	30,25	0,35	20	1,2042	12,7491	5,0	2,12	1,841E-05	2,0	2,77E+05	9,038569	0,54651	10,00	60,21	0,30	9,03121	0,150122
AM200x250_M05_0_040mps_a_SW2	5,0	30,25	0,40	20	1,2042	14,5704	5,0	2,42	1,841E-05	2,0	3,17E+05	12,18757	0,53788	10,00	60,21	0,30	9,03121	0,202424
AM200x250_M05_0_045mps_a_SW2	5,0	30,25	0,45	20	1,2042	16,3917	5,0	2,72	1,841E-05	2,0	3,56E+05	15,21505	0,54158	10,00	60,21	0,30	9,03121	0,252708

Table 4:   Test results with side-wind
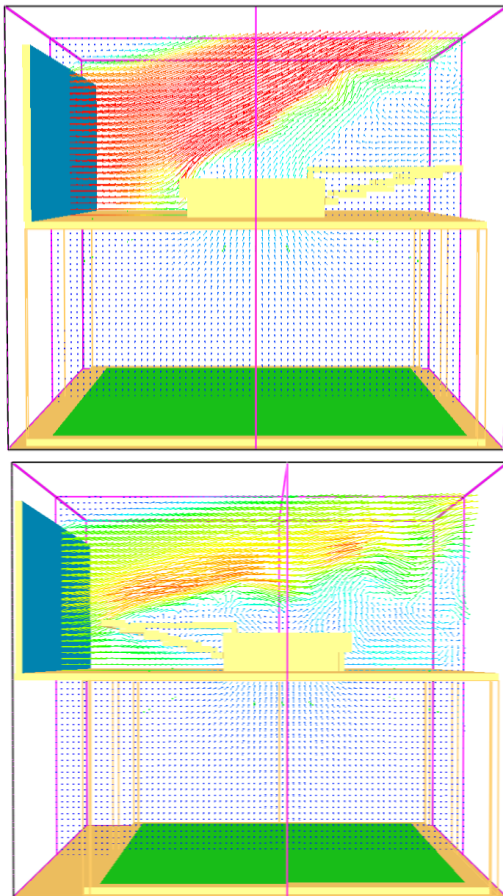
Figure 1,121: Velocity vectors around the side-wind model at side wind different angles

Based on the above diagram, when comparing the simulation result is C_v=0.622 with the value measured by the accredited laboratory (C_v=0,63), it may be stated that the simulation resulted in a very correct value.

5. SUMMARY

In this paper, only our method worked out for CFD simulation of roof smoke and heat vent domes with a proper size was described. By improving it further on, it may be made suitable to define the simulation method of facade smoke and heat vents, as well as louvred and lamellar smoke and heat vents opening up on two sides.

In our research, we have established that though the CFD technique is very laboursome with respect to

defining the C_v value, but regarding its accuracy, it may be compared with laboratory tests. The key establishment of our research is that for roof smoke and heat vents, the "Hole" element used in the simulation model shall be set by the geometrical cross-section of the vent to be used, but during this process, however, in order to simulate friction, footing of the natural smoke and heat vent as well as the floor thickness including the heat insulation shall be represented in the model environment. Further options for using the test method are as follows:

- carry out preliminary tests when developing new products and validate the actual test results;
- establish the actual C_v factor when installing roof smoke and heat vents of known C_v factor, strongly different from the test conditions (e.g. smoke and heat vent installed above a smoke-flue),
- test the effect that influences the efficiency for other active fire protection equipment (e.g. sprinkler heads installed below domes or their solar thermal collector dishes) added to roof smoke and heat ventilators of known C_v factor.

REFERENCES

[1]   Szikra Csaba: Engineering Methods in Smoke and Heat Extraction. Proceedings of ÉPKO, International Conference of Civil Engineering and Architecture 2013, Csíksomlyó, Romania, 15 June 2013., p. 313-319.

[2]   Szikra Csaba, Takács Lajos Gábor PhD: Practical Experiences of CFD Modelling in Smoke and Heat Spread Simulations. Proceedings of ÉPKO, International Conference of Civil Engineering and Architecture 2014, Csíksomlyó, Romania, 14 June 2014., p. 313-319.

[3]   EN 12101-2. Smoke and Heat Control Systems. Part 2: Specification for Natural Smoke and Heat Exhaust Ventilators

[4]   Fire Dynamic Simulator (Version 6) User's Guide. NIST Special Publication 1019-6, National Institute of Standards and Technology, U.S. Department of Commerce, 2013.

[5]   PyroSim User Manual. Thunderhead Engineering, 2013.